Eur. Phys. J. C (2024) 84:868
https://doi.org/10.1140/epjc/s10052-024-13219-1

THE EUROPEAN PHYSICAL JOURNAL C

Regular Article - Theoretical Physics

Compatibility of gravitational baryogenesis in $f(Q, C)$ gravity

Muhammad Usman[1,2,a], **Abdul Jawad**[1,3,b], **Abdul Malik Sultan**[4,c]

[1] Department of Mathematics, COMSATS University Islamabad, Lahore-Campus, Lahore 54000, Pakistan
[2] Department of Natural Sciences and Humanities, University of Engineering and Technology Lahore, New Campus, Lahore, Pakistan
[3] Institute for Theoretical Physics and Cosmology, Zhejiang University of Technology, Hangzhou 310023, China
[4] Department of Mathematics, University of Okara, Okara, Pakistan

Received: 26 April 2024 / Accepted: 5 August 2024

Abstract This paper investigates the disparity between matter and antimatter in the universe with the help of gravitational baryogenesis. This phenomenon commenced shortly after the big bang, resulting in a predominance of matter over antimatter. We analyze the mechanism of gravitational baryogenesis (baryon to entropy ratio) under the framework of $f(Q, C)$ gravity, where Q indicates non-metricity scalar and C denotes the boundary term. This Phenomenon depends on the charge parity violation interaction and for this paper we produce it with the coupling between baryon matter current (j^{ν}) and $\partial_{\nu}(Q + C)$. In the present work, we evaluate he baryon to entropy ratio $(\frac{\eta_B}{S})$ by proposing two models of $f(Q, C)$ with the assumption of power-law scale factor for each model and the universe contains perfect fluid throughout. We find that under optimal choice of model parameters, the results of $\frac{\eta_B}{S}$ of propose models in $f(Q, C)$ are compatible with the observational bound. The crux of the current work is that the outcomes of our propose models for generalized case of gravitational baryogenesis are consist with its observational constraint in different eras of the Universe.

1 Introduction

The surplus of matter compared to antimatter in our universe continues to stand as not only a significant enigma in the early universe but also one of the greatest puzzles in modern cosmological study. Alternatively, It is widely acknowledged the quantity of baryons throughout the Universe surpasses the amount of antibaryons [1,2]. Substantial cosmological evidence, along with various theoretical and empirical findings such as the big-bang nucleosynthesis (BBN) [3], cosmic microwave background (CMB) [4] and the annihilation of matter–antimatter [5], strongly indicate prevalence of matter over antimatter in our universe. The phenomenon by which matter supersedes antimatter is termed as baryogenesis. Scientists believe that shortly following the Big Bang, an imbalance arose among matter and antimatter, resulting in the minor conversion of antimatter into matter. Subsequently, the annihilation of matter and antimatter occurred, leading to an excess of matter that constitutes everything observable in our universe. However, the underlying cause of this asymmetry, known as "baryon asymmetry" (BA) remains elusive.

Sakharov [6], identified three fundamental criteria necessary for the generation of BA. These criteria are (i): process that violate baryon number, (ii): violation of charge (C) and charge parity (CP) symmetry and (iii): process out of the thermal equilibrium. Numerous intriguing and relevant mechanisms for generating BA that meet the specified criteria have been put forward. A theoretically appealing mechanism for triggering the asymmetry between matter and antimatter is "gravitational baryogenesis" [7]. Observational data [3,4] confirm that the ratio of baryon to entropy (i.e. $\frac{\eta_B}{S}$) is approximately equal to 9.42×10^{-11}, here S signifies the entropy of the universe while η_B denotes the baryon number.

The gravitational baryogenesis mechanism employs one of the Sakharov's criteria [7], the asymmetry between baryons and antibaryons is ensured by the presence of CP violation. The central element comprises a CP-violating interaction governed by the coupling between the baryon matter current j^{ν} and the derivative of the Ricci scalar curvature R expressed as

$$\frac{1}{M_*^2}\int \sqrt{-g}\, j^{\nu}(\partial_{\nu}R)d^4x,$$

where M_* represents the parameter that characterizes the cut-off scale of the underlying effective gravitational theory, and

[a] e-mails: usman.uet.lec@gmail.com; usman.math@uet.edu.pk
[b] e-mails: jawadab181@yahoo.com; abduljawad@cuilahore.edu.pk (corresponding author)
[c] e-mails: maliksultan23@gmail.com; ams@uo.edu.pk

Published online: 30 August 2024

g denotes the determinant of the metric tensor. Physicists have extended the above equation for different modified gravity theories [8–11]. This extension is motivated by the observation that other curvature invariants, like the Gauss–Bonnet (GB) scalar G, torsion scalar T, and non-metricity Q, leads to a BA that is not zero with radiation dominated universe $\omega = \frac{1}{3}$, a feature not achievable in general relativity (GR).

Hubble's measurements were the first to confirm that we inhabit an expanding universe that is also accelerating. Theoretical physics offers two main approaches to understand this expansion. The first one concerns dark energy (DE) incorporated into the right side of the Einstein field equations as described by GR. The second approach comprises modified gravity theories, which involve alterations to the left side of Einstein's field equations that stem from the Einstein–Hilbert action. The framework of modified gravity theories aims to provide a comprehensive description of the universe's history. This includes accommodating early and late-time acceleration, also ensuring compatibility with observational data [12–16]. Many authors worked on modified gravities as well as DE models and obtain feasible outcomes [17–27].

Modified gravity theories offer versatile tools for exploring various facts of the universe within the framework of modern cosmology including gravitational baryogenesis. The authors investigated the ratio of $\frac{\eta_B}{S}$ under the framework of the GB braneworld [28], they also analyzed the affect of the novel terms on $\frac{\eta_B}{S}$ and found feasible results. Gravitational baryogenesis was examined within the context of $f(R)$ gravity and obtained consistent outcomes [29–31]. Oikonomou examined how the baryogenesis process could potentially restrict with Type IV singularity [32]. In [33], authors investigated the baryogenesis with different choices of $f(T)$ gravity. Odintsov et al. obtained the compatible results of baryon number to entropy ratio with the observational data under the framework of loop quantum cosmology [34] and GB gravitational baryogenesis [9]. Goodarzi [2] employed the non-minimal derivative coupling model to explore gravitational baryogenesis and they found that BA produce under both high and low reheating temperatures by taking into account friction constraints.

The authors of [35,36] analyzed the baryon to entropy (BTE) ratio under the framework of $f(R, \mathcal{T})$, where $\mathcal{T}$ indicates the trace of energy momentum tensor and they found consistent outcomes with the observational data. The investigation of baryogenesis within the framework of $f(Q, \mathcal{T})$ where Q represents non-metricity along with the coupling $J^{\nu}\partial_{\nu}Q$ has been conducted yields findings aligned with observational consistency [11]. In [1], authors analyzed the generalized form of gravitational baryogenesis under the frameworks of $f(T, T_G)$ and $f(T, B)$, here T_G represents the teleparallel equivalent of the GB term and B signifies the boundary term between torsion and Ricci scalar. They formulated the BTE ratio with the scale factor of power law form for each model and confirm the consistency of their outcome with the observational value. The gravitational baryogenesis under the frameworks of $f(\mathcal{G}, \mathcal{T})$ and $f(R, \mathcal{G})$ were investigated using different models [37], they found that the value of $\frac{\eta_B}{S}$ for the models lies with the observational limits. The BA within the framework of $f(R, A)$ cosmology was analyzed in [38], where A represents the trace of anti-curvature tensor and they obtained results consistent with observational data. Jaybhaye et al. [39] analyzed the gravitational baryogenesis with one model under the framework of $f(R, L_m)$ and they found compatible outcome of $\frac{\eta_B}{S}$ with the observation bound. Jawad et al. [40] discussed the viability of baryogenesis constraints in modified Hŏrava–Lifshitz theory of gravity and found consistent results by constraining the model parameters.

The following structure is adopted in this article: Sect. 2 relates to summary of $f(Q, C)$ gravity and Friedmann equations, in Sect. 3 we discuss the gravitational baryogenesis in $f(Q, C)$ framework. We present BTE ratio for different models and discuss their outcomes in Sect. 4 while in Sect. 5 we discuss the generalized form of BTE ratio for different models and their outcomes. Section 6 relates to conclusions.

2 Review on $f(Q, C)$ gravity and field equations

Two feasible and interchangeable formulations of GR exist within spacetime without considering curvature where gravity can be entirely attributed to either the torsion or non-metricity properties of that spacetime. In the first scenario, an affine connection that is compatible with metric within flat spacetime featuring torsion replaces the unique torsion-free and metric-compatible Levi-Civita connection upon which GR was initially constructed, this specific theory initiated by Einstein himself [41] named as metric teleparallel theory. The second scenario gives rise to the symmetric teleparallel theory [42], developed from an affine connection characterized by zero curvature and torsion. Although both theories are tantamount to GR up to a boundary term, as both scalars T and Q are equivalent to the Levi-Civita Ricci scalar $\check{R}$. Recently, efforts have been undertaken to demonstrate the $f(\check{R})$ theory as a specific limit within both metric and symmetric teleparallel theories by integrating the corresponding boundary terms B and C into their Lagrangians. The $f(T, B)$ [43] and $f(Q, C)$ [44–46] theories so obtained are of the recent interest. The action corresponding to $f(Q, C)$ gravity is expressed as [44]

$$S = \int \left[\frac{1}{2k} f(Q, C) + L_m\right]\sqrt{-g}d^4x, \tag{1}$$

where L_m is a matter Lagrangian. The field equation is obtained on varying the action with respect to metric as follow [44]

$$kT_{bc} = -\frac{f}{2}g_{bc} + 2P^{\lambda}{}_{bc}\nabla_{\lambda}(f_Q - f_C) + \left(\check{G}_{bc} + \frac{Q}{2}g_{bc}\right)f_Q + \left(\frac{C}{2}g_{bc} - \check{\nabla}_b\check{\nabla}_c + g_{bc}\check{\nabla}^{\alpha}\check{\nabla}_{\alpha}\right)f_C. \tag{2}$$

Here, all the expressions with $(\check{})$ indicates the calculation with Levi-Civita connection $\check{\Gamma}$, tensor of superpotential is $P^{\lambda}_{bc} = \frac{1}{4}(-2L^{\lambda}{}_{bc} + Q^{\lambda}g_{bc} - \check{Q}^{\lambda}g_{bc} - \delta^{\lambda}{}_{(b}Q_{c)})$ and $L^{\lambda}{}_{bc} = \frac{1}{2}(Q^{\lambda}{}_{bc} - Q_{b}{}^{\lambda}{}_{c} - Q_{c}{}^{\lambda}{}_{b})$. The effective stress energy tensor is described as

$$T^{eff}_{bc} = T_{bc} + \frac{1}{k}\left(\frac{f}{2}g_{bc} - 2P^{\lambda}{}_{bc}\nabla_{\lambda}(f_Q - f_C) - \frac{Q}{2}g_{bc}f_Q - \left(\frac{C}{2}g_{bc} - \check{\nabla}_b\check{\nabla}_c + g_{bc}\check{\nabla}^{\alpha}\check{\nabla}_{\alpha}\right)f_C\right). \tag{3}$$

Therefore an equation resembling the GR is given by

$$\check{G} = \frac{k}{f_Q}T^{eff}_{bc}. \tag{4}$$

The additional component in Eq. (3) under cosmic context can be envisioned as a result of the geometric adjustments made while formulating the theory for generating a pseudo DE like component in $f(Q, C)$ as [44,45]

$$T^{DE}_{bc} = \frac{1}{f_Q}\left(\frac{f}{2}g_{bc} - 2P^{\lambda}{}_{bc}\nabla_{\lambda}(f_Q - f_C) - \frac{Q}{2}g_{bc}f_Q - \left(\frac{C}{2}g_{bc} - \check{\nabla}_b\check{\nabla}_c + g_{bc}\check{\nabla}^{\alpha}\check{\nabla}_{\alpha}\right)f_C\right). \tag{5}$$

The spacetime described by the FLRW metric is expressed through the line element in cartesian coordinates as below

$$ds^2 = -dt^2 + a^2(t)[dx^2 + dy^2 + dz^2], \tag{6}$$

where $a(t)$ is designated as the universe's scale factor and $H(t) = \frac{\dot{a}(t)}{a(t)}$ is known as Hubble parameter. Using vanishing affine connection $\Gamma^{\alpha}_{bc} = 0$ and get following necessary outcomes [44]

$$\check{R} = 6(2H^2 + \dot{H}), \quad Q = -6H^2, \quad C = \check{R} - Q = 6(3H^2 + \dot{H}). \tag{7}$$

Applying the above restrictions, therefore Friedmann-like equations are as given below [44]

$$k\rho = \frac{f}{2} + 6H^2 f_Q - (9H^2 + 3\dot{H})f_C + 3H\dot{f_C}, \tag{8}$$

$$kP = -\frac{f}{2} - (6H^2 + 2\dot{H})f_Q - 2H\dot{f_Q} + (9H^2 + 3\dot{H})f_C - \ddot{f_C}. \tag{9}$$

The $f(Q, C)$ gravity theory is recently introduced gravity theory, the theory avoids ghost degrees of freedom and matches with thermal history of the universe [44,45] that makes $f(Q, C)$ gravity a viable theory from a theoretical physics perspective. Therefore an obvious motivation is to analyze gravitational baryogenesis and its generalized form in this new gravity theory because it is a novel approach to handling non-metricity and coupling terms. This study will provides us the compatibility of BTE ratio with the observation bound for gravitational baryogenesis within the context of $f(Q, C)$ and its generalized form along with the comparative analysis with some latest pervious works for its effectiveness.

3 Gravitational baryogenesis in $f(Q, C)$

From the perspective of contemporary cosmology, the Big Bang explosion is believed to result in an equivalent generation of both matter and antimatter, leading to a net baryon number of zero. However, the observational data [3,4] and matter–antimatter annihilation [5] provide confirmation of a greater abundance of matter compared to antimatter in the universe. These observational methodologies offer a quantitative assessment of this asymmetry described by the dimensionless quantity [37,38]

$$\eta = \frac{\eta_B}{S} = \frac{\eta_B - \eta_{\bar{B}}}{S}, \tag{10}$$

where $\eta_B\,(\eta_{\bar{B}})$ represent the density of baryons (anti-baryons), and S denotes the entropy of the universe. The observed constraint on the BTE ratio is determined to be 9.42×10^{-11} [3,4,11]. This theoretical process, known as BA is associated with gravitational baryogenesis. For $f(Q, C)$ gravity, the interaction term that induces CP violation and give rise to the BA takes the following form

$$\frac{1}{M_*^2}\int \sqrt{-g}\, j^{\nu}\partial_{\nu}(Q + C)d^4x. \tag{11}$$

In the underlying scenario, the BTE ratio in $f(Q, C)$ gravity is given by

$$\frac{\eta_B}{S} \simeq -\frac{15g_b}{4\pi^2 g_{*s}}\frac{(\dot{Q} + \dot{C})}{M_*^2 T}\,|_{T=T_D} \simeq -\frac{15g_b}{4\pi^2 g_*}\frac{(\dot{Q} + \dot{C})}{M_*^2 T}\,|_{T=T_D}\,. \tag{12}$$

The gravitational baryogenesis emerges from the BA. Here T_D represents decoupling temperature. As the temperature of the universe decreased over its evolution and approaches a temperature lower than the decoupling temperature T_D (the temperature at which interactions generating BA start [39]) denoted as $T\,|_{T_D}$. The $g_b \sim O(1)$ denotes the inherent degree of freedom associated with baryons while g_{*s} indicates the overall degree of freedom for those particles which

contribute to the universe's entropy having very close value to the total degree of freedom of massless particles [29,47] i.e $g_{*s} = g_* \simeq 106$. To study the baryogenesis, consider that the thermal equilibrium holds and the energy density is proportional to the temperature T_D as below [1]

$$\rho(T) = \frac{\pi^2}{30} g_* T_D^4. \tag{13}$$

We consider power law solutions to examine the term $\frac{\eta_B}{S}$. Power law solutions are more beneficial and convenient for clarifying the entire cosmic evolution. Here, for each model we assume power law form of $a(t)$ (scale factor) and construct the baryon to entropy (BTE) ratio ($\frac{\eta_B}{S}$) under the framework of $f(Q, C)$ gravity. Therefore scale factor of the universe and Hubble parameter in this scenario are given by [1,29].

$$a(t) = a_0 t^p, \quad H(t) = \frac{p}{t}, \tag{14}$$

where p is a positive real constant [29] and $a_0(t)$ represents the current time value of scale factor. Using Eqs. (7), (12), (14) and after some simplifications, we get

$$\frac{\eta_B}{S} \simeq -\frac{45 g_b p(2p-1)}{\pi^2 g_* M_*^2 t^3 T_D}. \tag{15}$$

4 Baryon to entropy ratio for different models in $f(Q, C)$ gravity

In this section, we formulate the ratio of baryon to entropy relationships for gravitational baryogenesis within the framework of $f(Q, C)$ gravity theory. For each model we calculate the expressions of energy densities and the decoupling cosmic time that enable us a graphical analysis of BTE ratio (i.e $\frac{\eta_B}{S}$).

4.1 Model-1

First model is taken as

$$f(Q, C) = \beta Q + \alpha C^2, \tag{16}$$

where α and β are model parameter. The idea behind to propose this model in $f(Q, C)$ is that a similar type of power law model in the context of $f(T, B)$ was discussed in [48] and consider the article [49] that elaborates the viability of $f(Q)$ models. Using Eqs. (7), (8), (14), (16) and assuming $k = 1$, we get an expression for the energy density as

$$\rho = \frac{3p^2\left(\beta t^2 - 18\alpha(p+1)(3p-1)\right)}{t^4}. \tag{17}$$

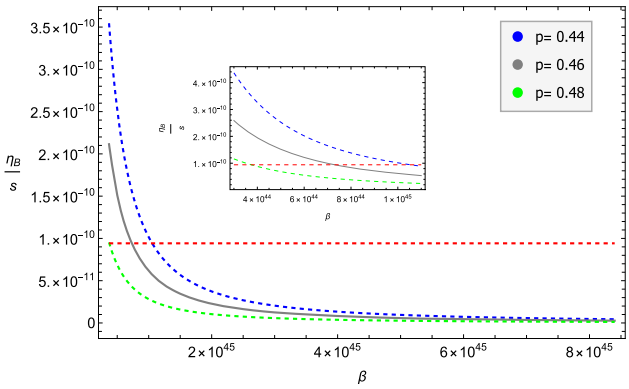

Fig. 1 Plot between ($\frac{\eta_B}{S}$) and (β) for model:1 having three distinct values of p with $g_b = 1, g_* = 106, M_* = 10^{12}$ GeV, $T_D = 2 \times 10^{16}$ GeV and $\alpha = -0.45 \times 10^{21}$

Using Eqs. (13) and (17), we derive an expression for the decoupling time t_D in terms of decoupling temperature T_D is given by the following

$$t_D = -\frac{1}{\sqrt{2\pi^2 g_* T_D^4}}\left(\left(8100\beta^2 p^4 - 4\pi^2 g_* T_D^4(4860\alpha p^4 + 3240\alpha p^3 - 1620\alpha p^2)\right)^{\frac{1}{2}} + 90\beta p^2\right)^{\frac{1}{2}}. \tag{18}$$

Therefor using Eqs. (15) and (18) the BTE ratio is given by

$$\frac{\eta_B}{S} \simeq \frac{45 g_b p(1-2p)}{\pi^2 g_* M_*^2 T_D \left(2\pi^2 g_* T_D^4\right)^{-\frac{3}{2}}}\left(90\beta p^2 + \left(8100\beta^2 p^4 - 4\pi^2 g_* T_D^4(4860\alpha p^4 + 3240\alpha p^3 - 1620\alpha p^2)\right)^{\frac{1}{2}}\right)^{-\frac{3}{2}}. \tag{19}$$

Figures 1 and 2 indicate the graphical behavior of ratio $\frac{\eta_B}{S}$ versus the parameter β and α respectively for model-1, the horizontal line (dashed line) represent the observational value of $\frac{\eta_B}{S} \simeq 9.42 \times 10^{-11}$ [3,4]. We consider the fixed constant values $g_b = 1, g_* = 106, M_* = 10^{12}$ GeV, $T_D = 2 \times 10^{16}$ GeV [1,11,37]. Plot between BTE ratio ($\frac{\eta_B}{S}$) and β with three choices of p is shown in Fig. 1, it is evident from the magnification of Fig. 1 that all the trajectories of $\frac{\eta_B}{S} \leq 9.42 \times 10^{-11}$ when $\beta > 1.1 \times 10^{45}$ and eventually meet with the observational value of horizontal line (red dashed line), this outcome consistent with the observational bound [3,4].

Plot for BTE ratio with respect to the parameter α with three different choices of p remains positive and $\frac{\eta_B}{S} \leq 9.42 \times 10^{-11}$ for $\alpha < -1.0 \times 10^{22}$ and finally all three trajectories of $\frac{\eta_B}{S}$ meet with observational value of $\frac{\eta_B}{S}$ as is evident from Fig. 2.

Following Table 1 indicates the behavior of different parameters of model-1 for baryogenesis. We see that

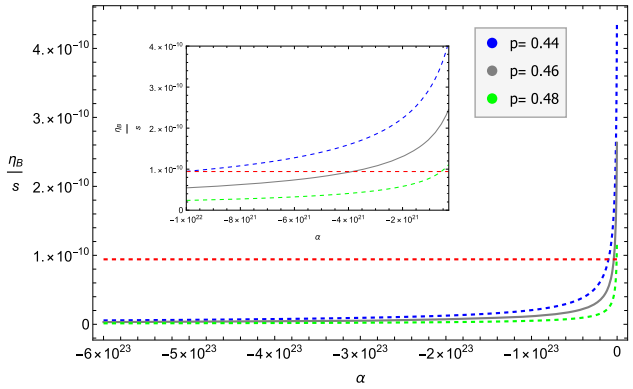

Fig. 2 Plot between $(\frac{\eta_B}{S})$ and (α) for model:1 having three distinct values of p with $g_b = 1, g_* = 106, M_* = 10^{12}$ GeV, $T_D = 2 \times 10^{16}$ GeV and $\beta = 3.5 \times 10^{44}$

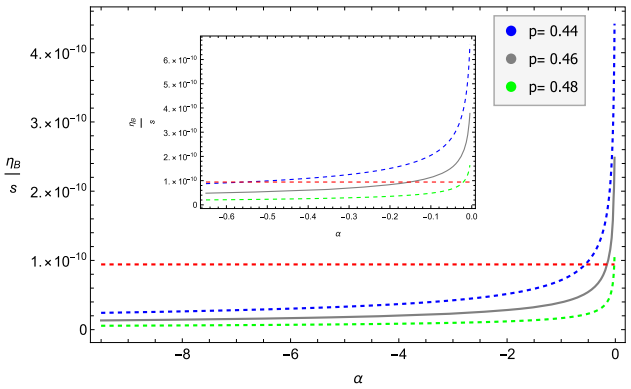

Fig. 3 Plot between $(\frac{\eta_B}{S})$ and (α) for model:2 having three distinct values of p with $g_b = 1, g_* = 106, M_* = 10^{12}$ GeV, $T_D = 2 \times 10^{16}$ GeV and $\beta = 0.2 \times 10^{45}$

Table 1 Behavior of different parameters for model-1 with $\frac{\eta_B}{S}$

α	β	p	$\frac{\eta_B}{S}$
-1.0×10^{22}	3.6×10^{44}	0.44	9.388×10^{-11}
-0.6×10^{22}	1.8×10^{44}	0.46	8.763×10^{-11}
-0.2×10^{22}	0.9×10^{44}	0.48	8.940×10^{-11}

the parameters α and p increases while the parameter β decreases to obtain the compatible values of $\frac{\eta_B}{S}$.

4.2 Model-2

For second model, we consider cubic form of boundary term as given below

$$f(Q, C) = \beta Q + \alpha C^3, \tag{20}$$

where α and β are model parameter. The energy density expression of model-2 is obtained using Eqs. (7), (8), (14) and (20) with $k = 1$ as follows

$$\rho = \frac{3p^2\left(\beta t^4 - 72\alpha(1-3p)^2 p(3p+5)\right)}{t^6}. \tag{21}$$

The expression for decoupling time t_D in the form of T_D is obtained using Eqs. (13) and (21) as given below

$$\begin{aligned} t_D = -\frac{1}{3\sqrt[3]{2}\pi^2 g_* T_D^4}\Big(&90\sqrt[3]{2}\beta p^2 + (2700\sqrt[3]{2}\beta^2 p^4) \\ &\times(\pi^2 T_D^4 g_*(1458000\beta^3 p^6 \\ &-874800\pi^4\alpha g_*^2 p^3 T_D^8 + 4723920\pi^4\alpha g_*^2 p^4 T_D^8 \\ &-4723920\pi^4\alpha g_*^2 p^5 T_D^8 - 4723920\pi^4\alpha g_*^2 p^6 T_D^8 \\ &+(-2125764000000\beta^6 p^{12} + (1458000\beta^3 p^6 \\ &-4723920\pi^4\alpha g_*^2 p^6 T_D^8 - 4723920\pi^4\alpha g_*^2 p^5 T_D^8 \\ &+4723920\pi^4\alpha g_*^2 p^4 T_D^8 - 874800\pi^4\alpha g_*^2 p^3 T_D^8)^2)^{\frac{1}{2}})^{\frac{1}{3}})^{-1} \\ &+(1458000\beta^3 p^6 - 874800\pi^4\alpha g_*^2 p^3 T_D^8 \\ &+4723920\pi^4\alpha g_*^2 p^4 T_D^8 - 4723920\pi^4\alpha g_*^2 p^5 T_D^8 \\ &-4723920\pi^4\alpha g_*^2 p^6 T_D^8 \\ &+(-2125764000000\beta^6 p^{12} + (1458000\beta^3 p^6 \\ &-874800\pi^4\alpha g_*^2 p^3 T_D^8 + 4723920\pi^4\alpha g_*^2 p^6 T_D^8 \\ &-4723920\pi^4\alpha g_*^2 p^5 T_D^8 - 4723920\pi^4\alpha g_*^2 p^4 \\ &\times T_D^8)^2)^{\frac{1}{2}})^{\frac{1}{3}}\Big)^{\frac{1}{2}}. \end{aligned} \tag{22}$$

Finally BTE ratio for this model has the following form

$$\frac{\eta_B}{S} \simeq -\frac{45 g_b p(2p-1)}{\pi^2 g_* M_*^2 t_D^3 T_D}, \tag{23}$$

where t_D is given by Eq. (22). For model 2 plot for $\frac{\eta_B}{S}$ with respect to the parameter α and β with three distinct values of p are shown in Figs. 3 and 4. In model 2 we assume the same values of fixed constant as used in model 1. Figure 3 implies that the three trajectories of ratio $\frac{\eta_B}{S}$ remains positive and less than 9.42×10^{-11} for $\alpha < -0.6$ and finally meet the horizontal dashed line (observational value $\frac{\eta_B}{S}$). In Fig. 4, the curves of ratio $\frac{\eta_B}{S}$ with three choices of p meet the observational value $\frac{\eta_B}{S}$ (horizontal dashed line) between $\beta \approx 0.7^{+0.6}_{-0.4} \times 10^{45}$ and magnification of this figure also signifies that $\frac{\eta_B}{S} \leq 9.42 \times 10^{-11}$ for $\beta > 1.1 \times 10^{45}$ which is a compatible outcome with the observational limits.

Following Table 2 signifies the behavior of different parameters of model 2 for baryogenesis. We see that the parameters α and p increases while the parameter β decreases to obtain the compatible values of $\frac{\eta_B}{S}$.

5 Generalized form of baryon to entropy ratio in $f(Q, C)$ gravity for different models

The more comprehensive form of gravitational baryogenesis interaction is regarded as generalized gravitational baryoge-

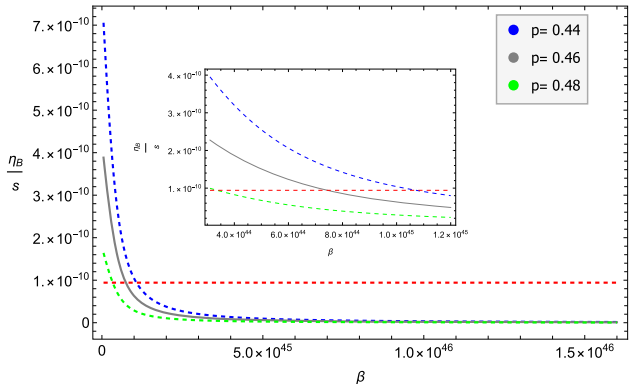

Fig. 4 Plot between $(\frac{\eta_B}{S})$ and (β) for model:2 having three distinct values of p with $g_b = 1, g_* = 106, M_* = 10^{12}$ GeV, $T_D = 2 \times 10^{16}$ GeV and $\alpha = -0.01$

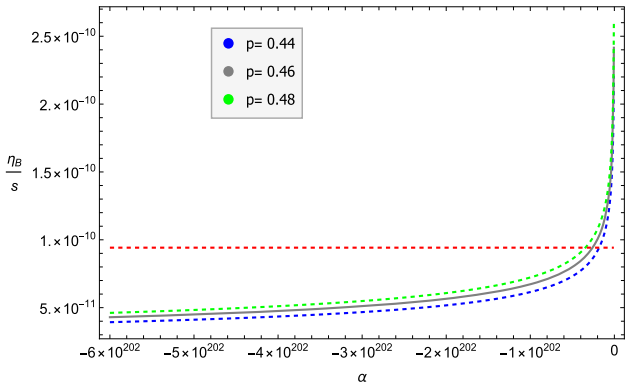

Fig. 5 Plot between $\frac{\eta_B}{S}$ and α for model:1 having three distinct values of p with $g_b = 1, g_* = 106, M_* = 10^{12}$ GeV, $T_D = 2 \times 10^{16}$ GeV and $\beta = 10$

Table 2 Behavior of different parameters for model 2 with $\frac{\eta_B}{S}$

α	β	p	$\frac{\eta_B}{S}$
-0.15	8.5×10^{44}	0.44	9.406×10^{-11}
-0.1	4.5×10^{44}	0.46	8.953×10^{-11}
-0.05	0.5×10^{44}	0.48	7.612×10^{-11}

nesis. In the context of generalized baryogenesis interaction, the CP-violating interaction is presented as follows

$$\frac{1}{M_*^2}\int \sqrt{-g}\, j^{\nu}\partial_{\nu} f(Q+C)d^4x. \tag{24}$$

In the underlying setup of generalized gravitational baryogenesis, BTE ratio is given by

$$\frac{\eta_B}{S} \simeq -\frac{15 g_b}{4\pi^2 g_*}\frac{(f_Q\ \dot{Q} + f_C\ \dot{C})}{M_*^2 T}\ |_{T=T_D}\ . \tag{25}$$

where $f_Q = \frac{\partial f}{\partial Q}$ and $f_C = \frac{\partial f}{\partial C}$. Next we discuss the BTE ratio of generalized gravitational baryogenesis for each model.

5.1 Model-1

The BTE ratio for generalized gravitational baryogenesis for model-1 is obtain by using Eqs. (7), (14), (16) and (25), as below

$$\frac{\eta_B}{S} \simeq \frac{45 g_b p^2 (12\alpha(1-3p)^2 - \beta t_D^2)}{\pi^2 g_* M_*^2 t_D^5 T_D}. \tag{26}$$

Using Eqs. (18) and (26), that yields the final form of the BTE ratio which is given below

$$\frac{\eta_B}{S} \simeq \frac{45 g_b p^2}{\pi^2 g_* M_*^2 T_D (2\pi^2 g_* T_D^4)^{\frac{3}{2}}} \times\Bigg(12\alpha(1-3p)^2(2\pi^2 g_* T_D^4) - \beta\Bigg(-90\beta p^2$$

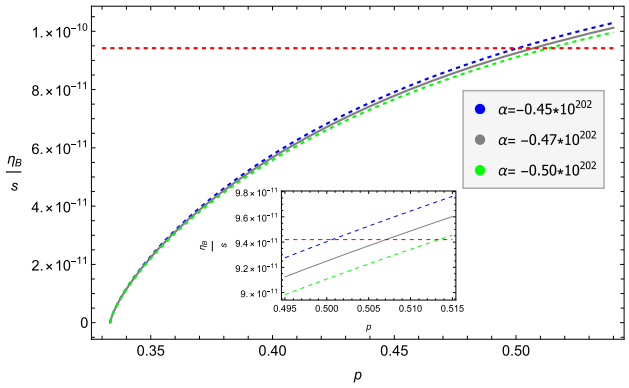

Fig. 6 Plot between $\frac{\eta_B}{S}$ and p for model:1 having three distinct values of α with $g_b = 1, g_* = 106, M_* = 10^{12}$ GeV, $T_D = 2 \times 10^{16}$ GeV and $\beta = 10$

$$+\Bigg(8100\beta^2 p^4 - 4(4860\alpha p^4 + 3240\alpha p^3 - 1620\alpha p^2)(\pi^2 g_* T_D^4)\Bigg)^{\frac{1}{2}}\Bigg)\Bigg) \times\Bigg(-90\beta p^2\Bigg(8100\beta^2 p^4 - 4(4860\alpha p^4 + 3240\alpha p^3 - 1620\alpha p^2)(\pi^2 g_* \times T_D^4)\Bigg)^{\frac{1}{2}}\Bigg)^{\frac{-5}{2}}. \tag{27}$$

Plot for BTE ratio with respect to α with three distinct values of p is shown in Fig. 5. The curves of BTE meet the dashed line (observation value of BTE ratio) between $-0.4 \times 10^{202} \leq \alpha \leq -0.006 \times 10^{202}$, further this fig implies that $\frac{\eta_B}{S}$ is positive and $\leq 9.42 \times 10^{-11}$ for $\alpha < -0.006 \times 10^{202}$ that indicate the consistent behavior with observational bound. Plot for $\frac{\eta_B}{S}$ with respect to p with three distinct values of α is shown in Fig. 6. This figure indicates that all the three curves meet the observation value of BTE between $0.5 \leq p < 0.515$.

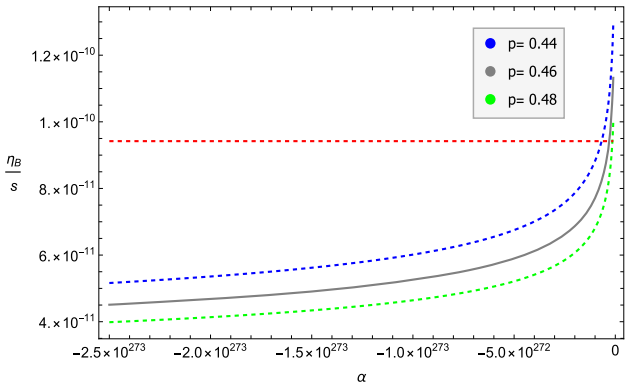

Fig. 7 Plot between $\frac{\eta_B}{S}$ and α for model:2 having three distinct values of p with $g_b = 1$, $g_* = 106$, $M_* = 10^{12}$ GeV, $T_D = 2 \times 10^{16}$ GeV and $\beta = 10$

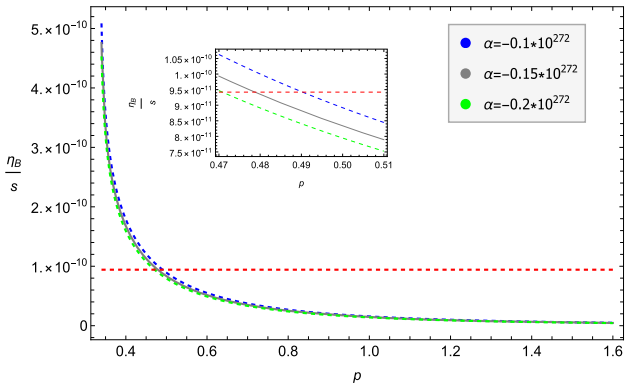

Fig. 8 Plot between $\frac{\eta_B}{S}$ and p for model:2 having three distinct values of α with $g_b = 1$, $g_* = 106$, $M_* = 10^{12}$ GeV, $T_D = 2 \times 10^{16}$ GeV and $\beta = 10$

5.2 Model-2

The BTE ratio of model-2 for generalized gravitational baryogenesis is obtain with the help of Eqs. (20) and (25) as below

$$\frac{\eta_B}{S} \simeq \frac{45 g_b p^2 (108\alpha p(3p-1)^3 - \beta t_D^4)}{\pi^2 g_* M_*^2 t_D^7 T_D}, \tag{28}$$

where t_D is given by Eq. (22). Figure 7 shows the plot between $\frac{\eta_B}{S}$ for generalized gravitational baryogenesis of model-2 with respect to α. This figure indicates that all three trajectories of $\frac{\eta_B}{S}$ have positive values and meet the observational value (horizontal line) between $-1 \times 10^{272} \leq \alpha < -0.1 \times 10^{272}$. Plot of BTE ratio with respect to p is shown in Fig. 8 with three distinct choices of α. It reveals from Fig. 8 that the value of $\frac{\eta_B}{S}$ remains positive and their trajectories meet the observation value of $\frac{\eta_B}{S}$ (horizontal dashed line) in the range $0.47 \leq p < 0.5$.

6 Conclusions

In the present paper, we have explored the mechanisms of gravitational baryogenesis and generalized gravitational baryogenesis under the framework of $f(Q, C)$ gravity theory. The concept of gravitational baryogenesis was first introduced by Davoudiasl et al. [7]. They formulated this concept by examining CP-violation with the coupling between the Ricci scalar and the current of baryon matter. The $f(Q, C)$ gravity is newly proposed gravity where f denotes a smooth function of the non-metricity scalar Q and the associated boundary term C [44,45]. The BTE ratio $\frac{\eta_B}{S}$ depends on CP-violation interaction, for the current framework it is produced with the coupling between baryon matter current (j^ν) and $\partial_\nu(Q + C)$ for baryogenesis and coupling between (j^ν) and $\partial_\nu f(Q + C)$ for generalized form of gravitational baryogenesis. To investigate the mentioned mechanisms in $f(Q, C)$, we have analyzed the ratio $\frac{\eta_B}{S}$ of two propose models with the assumption of the scale factor of the power law form $(a = a_0 t^p)$ and compare our outcomes with the observational value of $\frac{\eta_B}{S}$ [3,4]. Following are the core outcomes of this research work:

- Model-1: Fig. 1 shows the graphical behavior of $\frac{\eta_B}{S}$ against β, all three trajectories meet with the observation value of $\frac{\eta_B}{S}$ between $0.35 \times 10^{45} \leq \beta \leq 1.5 \times 10^{45}$, Fig. 2 implies that BTE ratio satisfies $0 \leq \frac{\eta_B}{S} < 9.42 \times 10^{-11}$ for $\alpha < -1.0 \times 10^{-22}$, these are compatible behavior with respect to observational bound. Figures 5 and 6 show the the graphical outcome of $\frac{\eta_B}{S}$ w.r.t α and p for generalized gravitational baryogenesis. These figures respectively demonstrate that BTE ratio lies within $0 \leq \frac{\eta_B}{S} < 9.42 \times 10^{-11}$ for $\alpha < -0.006 \times 10^{202}$ and all three trajectories of BTE meet to its observation value i.e $\frac{\eta_B}{S} \approx 9.42 \times 10^{-11}$ in the range $0.5 \leq p < 0.515$. Since for each model, we use scale factor of the power law form $(a = a_0 t^p)$, there exists a relation between p and ω (EoS parameter for different eras of the universe) $p = \frac{2}{3(1+\omega)}$ [39], since this model is good agreement with the observational value of $\frac{\eta_B}{S}$ at $p = 0.5$, for $p = 0.5$ then $\omega = \frac{1}{3}$ which implies that model-1 indicates compatible behavior in radiation dominated era.
- Model-2: The graphical response for baryogenesis of model-2 for $\frac{\eta_B}{S}$ w.r.t α, β is shown in Figs. 3 and 4. These figures indicate that $0 \leq \frac{\eta_B}{S} < 9.42 \times 10^{-11}$ for $\alpha < -0.6$ and the curves of $\frac{\eta_B}{S}$ meet to its observation value between $\beta \approx 0.7^{+0.6}_{-0.4} \times 10^{45}$ respectively. The graphical working for $\frac{\eta_B}{S}$ w.r.t α, p visible in Figs. 7 and 8 for generalized form of gravitational baryogenesis. Plot of $\frac{\eta_B}{S}$ w.r.t α coincide with the observation value for $-1 \times 10^{272} \leq \alpha < -0.1 \times 10^{272}$, while all three plots of $\frac{\eta_B}{S}$ w.r.t p meet to its observational value within

$0.47 \leq p < 0.5$ and for $0.5 \geq p \geq 1.6$, the ratio $\frac{\eta_B}{S}$ remains positive and less than 9.42×10^{-11}. According to relation $p = \frac{2}{3(1+\omega)}$ [39], this model shows consistent behavior of generalized gravitational baryogenesis in all three eras i.e radiation, matter dominant as well as quintessence era.

Additionally, We have observed that the proposed model-2 in theoretical framework of $f(Q, C)$ gravity is better for the viability testing of the phenomenon of generalized gravitational baryogenesis because $\frac{\eta_B}{S}$ remains positive (non-zero BA) and less than the observational upper bound in matter as well as quintessence era, and eventually $\frac{\eta_B}{S}$ meets with the observation limit in radiation era. For the comparative analysis of this outcome with some pervious works [37,39] where the same assumption of scale factor is used to analyze the generalized gravitational baryogenesis in the context of different gravity frameworks, we deduce that the authors of [39] analyzed this phenomenon in radiation dominant era only, while the authors of [37] analyzed the phenomenon with the large values of model parameters and obtain good match with observation limit of $\frac{\eta_B}{S}$ in quintessence and phantom era, on the other hand our model-2 is compatible with the observational bound of $\frac{\eta_B}{S}$ in radiation, matter as well as quintessence era.

Acknowledgements Abdul Jawad is thankful to ITPC and Zheijiang University of Technology for providing the postdoctoral opportunity.

Data Availability Statement My manuscript has no associated data. [Authors' comment: Data sharing not applicable to this article as no datasets were generated or analysed during the current study.]

Code Availability Statement My manuscript has no associated code/software. [Authors' comment: Code/Software sharing not applicable to this article as no code/software was generated or analysed during the current study.]

Funded by SCOAP[3].

References

1. N. Azhar, A. Jawad, S. Rani, Phys. Dark Univ. **30**, 100724 (2020)
2. P. Goodarzi, Eur. Phys. J. C **83**, 990 (2023)
3. S. Burles, K.M. Nollett, M.S. Turner, Phys. Rev. D **63**, 063512 (2001)
4. D.N. Spergel et al. WMAP Collaboration, Astrophys. J. Suppl. **170**, 377 (2007)
5. A.G. Cohen, A. Rujula De, S.L. Glashow, Astrophys. J. **495**, 539 (1998)
6. A.D. Sakharov, JETP Lett. **5**, 24 (1967)
7. H. Davoudiasl et al., Phys. Rev. Lett. **93**, 201301 (2004)
8. G. Lambiase, G. Scarpetta, Phys. Rev. D **74**, 087504 (2006)
9. S.D. Odintsov, V.K. Oikonomou, Phys. Lett. B **760**, 259 (2016)
10. V.K. Oikonomou, E.N. Saridakis, Phys. Rev. D **94**, 124005 (2016)
11. S. Bhattacharjee, P.K. Sahoo, Eur. Phys. J. C **80**, 289 (2020)
12. T. Clifton et al., Phys. Rep. **513**, 1 (2012)
13. S. Nojiri, S.D. Odintsov, Int. J. Geom. Methods Mod. Phys. **04**, 115 (2007)
14. S. Nojiri, S.D. Odintsov, Phys. Rep. **505**, 59 (2011)
15. E.J. Copeland, M. Sami, S. Tsujikawa, Int. J. Mod. Phys. D **15**, 1753 (2006)
16. Y.F. Cai et al., Rep. Prog. Phys. **79**, 106901 (2016)
17. S. Capozziello et al., Phys. Lett. B **639**, 135 (2006)
18. S. Nojiri, S.D. Odintsov, Phys. Rev. D **74**, 086005 (2006)
19. A.A. Starobinsky, JETP Lett. **86**, 15 (2007)
20. S. Nojiri, S.D. Odintsov, Phys. Lett. B **631**, 1 (2005)
21. T. Harko et al., Phys. Rev. D **84**, 024020 (2011)
22. A. Sheykhi, S. Ghaffari, H. Moradpour, Int. J. Mod. Phys. D **28**, 1950080 (2019)
23. M. Usman, A. Jawad, Eur. Phys. J. C **83**, 958 (2023)
24. S. Nojiri, S.D. Odintsov, E.N. Saridakis, Eur. Phys. J. C **79**, 242 (2019)
25. S. Mandal, D. Wang, P.K. Sahoo, Phys. Rev. D **102**, 124029 (2020)
26. S. Nojiri, S.D. Odintsov, V.K. Oikonomou, Phys. Rep. **692**, 1–104 (2017)
27. M. Usman, A. Jawad, Int. J. Mod. Phys. D **32**, 2350100 (2023)
28. M.C. Bento et al., Phys. Rev. D **71**, 123517 (2005)
29. G. Lambiase, G. Scarpetta, Phys. Rev. D **74**, 087504 (2006)
30. M.P.L.P. Ramos, J. Paramos. Phys. Rev. D **96**, 104024 (2017)
31. X. Xiang, J. Zhou, Y. Deng, X. Yang, Identifying the generator matrix of a stationary Markov chain using partially observable data. Chaos Interdiscipl. J. Nonlinear Sci. **34**(2), 023132 (2024). https://doi.org/10.1063/5.0156458
32. V.K. Oikonomou, Int. J. Geom. Methods Mod. Phys. **13**, 1650033 (2016)
33. V.K. Oikonomou, E.N. Saridakis, Phys. Rev. D **94**, 124005 (2016)
34. S.D. Odintsov, V.K. Oikonomou, Europhys. Lett. **116**, 49001 (2016)
35. E.H. Baffou, M.J.S. Houndjo, D.A. Kanfon, I.G. Salako, Eur. Phys. J. C **79**, 112 (2019)
36. P.K. Sahoo, S. Bhattacharjee, Int. J. Theor. Phys. **59**, 1451 (2020)
37. N. Azhar, A. Jawad, S. Rani, Phys. Dark Univ. **32**, 100815 (2021)
38. A. Jawad, A.M. Sultan, EPL **138**, 29001 (2022)
39. L.V. Jaybhaye, S. Bhattacharjee, P.K. Sahoo, Phys. Dark Univ. **40**, 101223 (2023)
40. A. Jawad, A.M. Sultan, S. Rani, Symmetry **15**, 824 (2023)
41. A. Unzicker, T. Case, arXiv:physics/0503046 (2005)
42. J.M. Nester, H.J. Yo, Chin. J. Phys. **37**, 113 (1999)
43. S. Bahamonde et al., Phys. Rev. D **92**, 104042 (2015)
44. G.N. Gadbail, A. De, P.K. Sahoo, Eur. Phys. J. C **83**, 1099 (2023)
45. A. De, T.-H. Loo, E.N. Saridakis, JCAP **03**, 050 (2023)
46. S. Capozziello, V. De Falco, C. Ferrara, Eur. Phys. J. C **83**, 915 (2023)
47. S. Rani, A. Javed, A. Jawad, Eur. Phys. J. Plus **138**, 5 (2023)
48. C. Escamilla-Rivera, J.L. Said, Class. Quantum Gravity **37**, 16 (2020)
49. A. De, T.H. Loo, Class. Quantum Gravity **40**, 115007 (2023)